European Journal of Neuroscience, Vol. 26, pp. 250–260, 2007 doi:10.1111/j.1460-9568.2007.05634.x

Coding of movement- and force-related information in primate primary motor cortex: a computational approach

Emmanuel Guigon,[1] Pierre Baraduc[2] and Michel Desmurget[2]
[1]INSERM U742, ANIM, Université Pierre et Marie Curie (UPMC – Paris 6), 9, quai Saint-Bernard, 75005 Paris, France
[2]Centre de Neurosciences Cognitives, CNRS UMR 5229, 67, Bd Pinel, 69675 Bron, France

Keywords: computer, control, force, muscle, neuron

Abstract

Coordinated movements result from descending commands transmitted by central motor systems to the muscles. Although the resulting effect of the commands has the dimension of a muscular force, it is unclear whether the information transmitted by the commands concerns movement kinematics (e.g. position, velocity) or movement dynamics (e.g. force, torque). To address this issue, we used an optimal control model of movement production that calculates inputs to motoneurons that are appropriate to drive an articulated limb toward a goal. The model quantitatively accounted for kinematic, kinetic and muscular properties of planar, shoulder/elbow arm-reaching movements of monkeys, and reproduced detailed features of neuronal correlates of these movements in primate motor cortex. The model also reproduced qualitative spatio-temporal characteristics of movement- and force-related single neuron discharges in non-planar reaching and isometric force production tasks. The results suggest that the nervous system of the primate controls movements through a muscle-based controller that could be located in the motor cortex.

Introduction

Motor control is central to executive functions of the nervous system. It guarantees that planned actions are efficiently translated into appropriate limb displacements. A striking feature of this translation from 'ideas of motion' to 'mechanical motion' is the paradoxical contrast between the apparent easiness with which movements are performed on the one hand, and the complexity of Newtonian dynamics and the existence of multiple levels of redundancy on the other (Bernstein, 1967). Since the time of Bernstein, this paradox has been copiously documented and solutions have been proposed to explain how the nervous system can solve such a challenging problem (Bullock & Grossberg, 1988; Uno *et al*., 1989; Kalaska & Crammond, 1992; Harris & Wolpert, 1998; Todorov & Jordan, 2002; Guigon *et al*., 2007). Yet the central issue of the nature of neural control signals (NCSs) that flow from central motor systems to the periphery during coordinated movements remains open and hotly debated (Kalaska *et al*., 1989; Caminiti *et al*., 1991; Fetz, 1992; Feldman & Levin, 1995; Georgopoulos, 1996; Kakei *et al*., 1999; Georgopoulos & Ashe, 2000; Moran & Schwartz, 2000; Todorov, 2000, 2003; Scott, 2005; Aflalo & Graziano, 2006).

A common method to address this issue is to record NCSs *in vivo*, e.g. using single-unit recordings in the primary motor cortex (M1) and spinal cord of behaving animals (monkeys), and to perform a correlation analysis in order to reveal preferential relationships between discharge rates and parameters of motor behaviour (e.g. direction of movement, velocity, joint torques; Evarts, 1968; Georgopoulos *et al*., 1982; Kalaska *et al*., 1989; Moran & Schwartz, 1999). This method has revealed a large repertoire of discharge patterns as well as a large repertoire of correlations that were thought to reflect sometimes kinematic (direction, velocity), sometimes dynamic (forces) representations of motor acts. However, these correlations were time-varying and complex (Ashe & Georgopoulos, 1994; Fu *et al*., 1995), and were in general contaminated by real or apparent covariations among parameters (Mussa-Ivaldi, 1988; Todorov, 2000; Scott, 2005). Furthermore, as correlations do not imply causality, neurophysiological data are not sufficient to draw firm conclusions on this issue.

A complementary approach is to define the requisite characteristics of NCSs based on a model of motor control, and to compare requisite and actual properties of these signals (Lan, 1997; Bullock *et al*., 1998; Todorov, 2000; Haruno & Wolpert, 2005). Here we exploit an optimal control model that quantitatively accounts for kinematic and dynamic properties of redundant manipulators (Guigon *et al*., 2007) to address the nature of NCSs generated by the nervous system to control arm-reaching movements.

Materials and methods

Scope of the model

To properly ascertain the contribution of neural activities to movement control, it is necessary to consider neural and movement data simultaneously. An appropriate animal (monkey) model of this situation is obtained using a mechanical exoskeleton that puts constraints on the degrees of freedom (DOF) involved in the movement (Scott *et al*., 2001; Graham *et al*., 2003; Kurtzer *et al*., 2006). In this case, the mechanical apparatus can be represented by a planar two-joint arm. In other studies of interest (Caminiti *et al*., 1991; Sergio & Kalaska, 1998; Kakei *et al*., 1999; Sergio *et al*., 2005), the movements involved more than 2 DOF. In theory, the model could be used to address these experiments (Guigon *et al*., 2007). However, not enough kinematic and kinetic data are available in these studies for a

Correspondence: Dr E. Guigon, as above.
E-mail: guigon@ccr.jussieu.fr

Received 2 January 2007, revised 6 April 2007, accepted 17 May 2007

thorough comparison between experimental observations and predictions of the model. Accordingly, we thoroughly and quantitatively addressed the neural control of planar two-joint arm movements. In this framework, we also reproduced qualitative aspects of motor cortical discharge related to non-planar arm-reaching movements (Sergio & Kalaska, 1998; Sergio *et al*., 2005).

The model described in this article is formally identical to the model used in Guigon *et al*. (2007). Yet the two articles address complementary issues. In the previous article, we described predicted kinematic and dynamic characteristics of upper limb movements. Here, we focus on the nature of the predicted control signals (CSs) that are responsible for these movements. For clarity, we give below a brief overview of the model, but a thorough presentation can be found in Guigon *et al*. (2007).

Overview of the model

In a schematic view of motor control, a cortical motor centre sends a command to a neuromuscular apparatus (motoneuron + muscle), which generates a force to displace a set of articulated segments. Formally, this series of events can be represented by the action of a 'controller' upon a 'controlled object'. Mathematically, the behaviour of the controlled object can be described by a state-dependent dynamics:

$$\mathrm{d}\mathbf{x}/\mathrm{d}t = f(\mathbf{x}(t),\ \mathbf{u}(t)), \tag{1}$$

where $\mathbf{x}$ is the state vector of the object (position, velocity, muscle state, …), and $\mathbf{u} = \{u_i\}$ ($1 \le i \le M$, M number of muscles) the control vector (or CS) transmitted by the controller. A control problem corresponds to the mastering of the controlled object, i.e. find a time series of control $\mathbf{u}(t)$ (t in $[t_0; t_f]$) in order to satisfy to constraints of a *task*, e.g.

$$\mathbf{x}(t_0) = \mathbf{x}_0 \text{ and } \psi(\mathbf{x}(t_f)) = 0, \tag{2}$$

where function ψ expresses constraints on the final state of the object.

Once the control problem is solved, the quantities $\mathbf{x}(t)$ and $\mathbf{u}(t)$ can be analysed and compared with corresponding quantities obtained in experimental studies: position/velocity to movement kinematics; force/torque to movement dynamics; control to cortical activity.

In the framework of this study, an appropriate controller should meet the following requirements: (i) to provide a unique solution in the face of spatial, temporal, kinematic and muscular redundancy; (ii) to provide a solution that has realistic kinematic characteristics. We have shown previously that a controller that chooses, among solutions to Eqns (1) and (2), the unique solution that minimizes overall control magnitude (E, effort):

$$E^2 = \int_{[t_0;t_f]} ||\mathbf{u}(t)||^2 \mathrm{d}t, \tag{3}$$

where $||\mathbf{u}(t)||$ is the norm of vector $\mathbf{u}$, complies with these requirements (Guigon *et al*., 2007). Technically, $\mathbf{u}$ is the solution of an optimal control problem. Because the focus of this article is the issue of the nature of NCSs that are elaborated by the nervous system to produce coordinated movements, we do not intend here to show that this controller is more realistic or efficient than other controllers. The fact that results described below could be obtained with other controllers is not at all detrimental to our purpose.

In general, Eqn (1) includes both dynamic (inertial, velocity-dependent) and static (elastic, gravitational) forces. A series of arguments (reviewed in Guigon *et al*., 2007) suggests that the nervous systems process the two types of force separately (separation principle), i.e.

$$\mathbf{u}(t) = \mathbf{u}_{\mathrm{dyn}}(t) + \mathbf{u}_{\mathrm{stat}}(t),$$

where $\mathbf{u}_{\mathrm{dyn}}(t)$ is the solution to the optimal control problem without static forces, and $\mathbf{u}_{\mathrm{stat}}(t)$ compensates for applied static forces. In the following, we only address the nature of dynamic CSs, in the absence of static forces, and $\mathbf{u}$ corresponds to $\mathbf{u}_{\mathrm{dyn}}$.

The controller is described here as an open-loop controller. However, it should be noted that the model is affiliated with a principled approach to motor control that states that feedback is a necessary component of an appropriate neural controller (Guigon *et al*., 2007). Thus, the controller can be considered as an optimal feedback controller, i.e. a controller that calculates the appropriate command to reach a goal for any estimate of the state of the controlled system (see also Scott, 2004; Todorov, 2004). Such a model can work properly in the presence of noise in sensory and motor pathways, and perturbations on limb or target position (Todorov & Jordan, 2002; Guigon *et al*., 2007). In practice, the feedback component remains hidden, as neither perturbations nor noise were introduced in the simulations. The results described below can be considered as mean data over noise distributions.

Controlled object

The controlled object was a planar, two-joint (shoulder, elbow) arm actuated by two pairs of monoarticular muscles and one pair of biarticular muscles (Fig. 1A). For each muscle, the actual force F was calculated following Zajac (1989) and Brown *et al*. (1996). We used:

$$F = \Gamma \times \mathrm{PCSA} \times F_{\mathrm{a}}(u) \times (F_{\mathrm{V}} \times F_{\mathrm{L}} + F_{\mathrm{P}}), \tag{4}$$

where: u is a control input (component of vector $\mathbf{u}$ for the corresponding muscle); Γ is a tension scaling factor; PCSA is the physiological cross-sectional area; F_{a} is a unitless quantity derived from muscle input:

$$\begin{aligned} F_{\mathrm{a}} &= \eta(a); \\ \upsilon\, \mathrm{d}a/\mathrm{d}t &= -a + e \\ \upsilon\, \mathrm{d}e/\mathrm{d}t &= -e + u \end{aligned} \tag{5}$$

where a and e are muscle activation and excitation, $\eta(z) = [z]^+$ ($[z]^+ = z$ if $z > 0$, otherwise $[z]^+ = 0$), υ is a parameter; F_{P} reflects passive forces:

$$\mathrm{F_P} = c_2\{\exp[k_2(L - L_{\mathrm{r2}})] - 1\}$$

where L is the normalized muscle length (the normalization factor is the length L_0 at which maximal isometric force is generated), c_2, k_2, L_{r2} are parameters; F_{L} and F_{V} are related to force–length and force–velocity curves of the muscle,

$$F_{\mathrm{L}} = \exp\{-[(L^{\beta} - 1)/\omega]^{\rho}\}$$

$$F_{\mathrm{V}} = (b_1 - a_1 V)/(V + b_1) \quad \text{if } V < 0 \text{ (shortening muscle)}$$

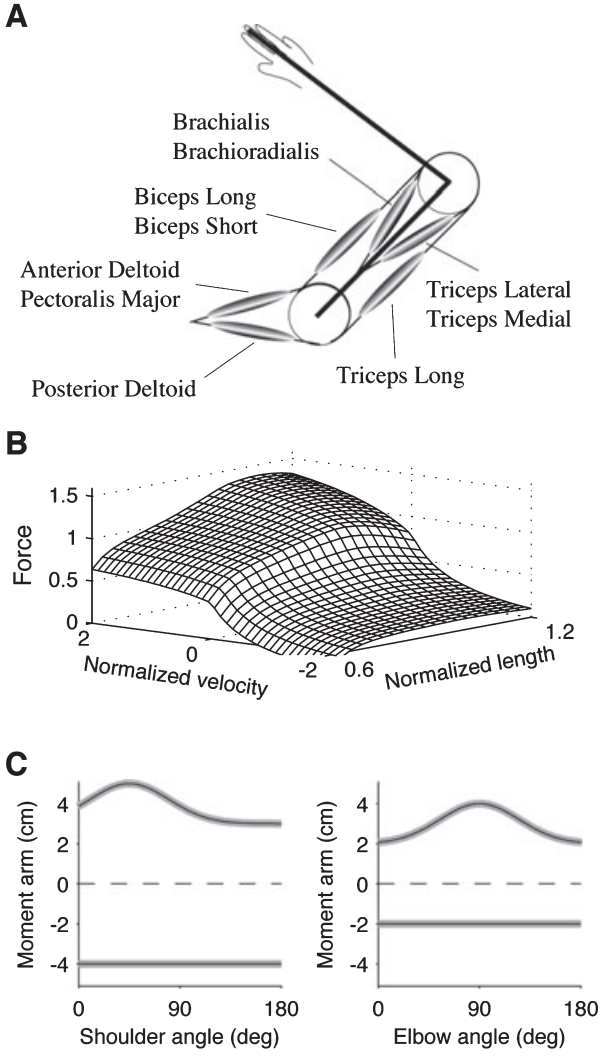

FIG. 1. (A) Model of a planar, two-joint arm equipped with two pairs of monoarticular antagonist muscles, and one pair of biarticular muscles. Muscle names are indicated for correspondence with the study of Kurtzer *et al.* (2006). (B) Length–velocity force curve. (C) Moment arms at shoulder (left) and elbow (right) for the monoarticular (thin black line) and biarticular (thick grey lines) muscles (positive for flexors; negative for extensors).

$$F_V = (b_2 - a_2 V)/(V + b_2) \quad \text{if } V > 0 \text{ (lengthening muscle)}$$

where V is the normalized muscle velocity (in units of L_0/s); β, ω, ρ, a_1, b_1, a_2, b_2 are parameters. The quantity $F_V \times F_L + F_P$ is plotted as a function of L and V in Fig. 1B (fig. 11B in Brown *et al.*, 1996).

The muscle forces were translated into joint torques according to:

$$T_{sh} = (\gamma_{sh}{}^{FL} \times F_{sh}{}^{FL}) - (\gamma_{sh}{}^{EX} \times F_{sh}{}^{EX}) + (\gamma_{bish}{}^{FL} \times F_{bi}{}^{FL}) - (\gamma_{bish}{}^{EX} \times F_{bi}{}^{EX})$$

$$T_{el} = (\gamma_{el}{}^{FL} \times F_{el}{}^{FL}) - (\gamma_{el}{}^{EX} \times F_{el}{}^{EX}) + (\gamma_{biel}{}^{FL} \times F_{bi}{}^{FL}) - (\gamma_{biel}{}^{EX} \times F_{bi}{}^{EX})$$

where $\gamma_{xx}{}^{YY}$ are the moment arms of the muscle, with xx = {sh, el, bi, bish, biel} and YY = {FL, EX}; sh = shoulder, el = elbow, bi = biarticular, FL = flexor, EX = extensor.

The controlled object contains two elements that are thought to play an important role in motor control: (i) force–length and force–velocity relationships in muscles (Todorov, 2000); (ii) biarticular muscles (van Bolhuis *et al.*, 1998). To address the influence of these elements in the framework of this study, we considered two modified versions of the model: (i) a model (NOLV) without force–length and force–velocity relationships in the muscles [i.e. $F = \Gamma \times \text{PCSA} \times F_a$ in Eqn (4)]; (ii) a model (NOBI) without biarticular muscles ($\gamma_{bi}{}^{**} = 0$).

NCSs

The control problem [Eqns (1–3)] was modified to account for the fact that there are many more neurons potentially involved in motor commands than muscles. We assumed that: (i) the number s of CSs was larger than the number M of muscles; (ii) each CS was defined by a fixed synergy of muscles [Eqn (7)]; (iii) the s synergies were uniformly distributed in muscular space [Eqn (7)]. Formally, the problem was similar to the problem defined by Eqns (1–3), with the following change. The goal was to find minimum control $\mathbf{U}(t) = \{U_j(t)\}$ $(1 \le j \le s)$, i.e. the unique solution that minimizes:

$$E_2 = \int_{[t_0;t_f]} || \mathbf{U}(t)||^2 \mathrm{d}t, \tag{6}$$

and is appropriate to displace the articulated segments between given initial and final positions, the muscular control vector $\mathbf{u}(t) = \{u_i(t)\}$ $(1 \le i \le M)$ being defined by:

$$u_i(t) = \sum_{j=1 \ldots s} \beta_{ij} U_j(t), \tag{7}$$

where β_{ij} are random coefficients drawn from a uniform distribution in [−1; 1]. The CSs $\{U_j(t)\}$ are called NCSs.

Tasks

To simulate arm movements, the torques (T_{sh}, T_{el}) were translated into displacements using the dynamics of the articulated segments (Newtonian dynamics; Guigon *et al.*, 2007). The control vector was:

$$\mathbf{u}(t) = [u_1, u_2, u_3, u_4, u_5, u_6]$$

i.e. the control for the shoulder flexor, shoulder extensor, elbow flexor, elbow extensor, biarticular flexor, biarticular extensor, in this order. For a 'movement' task, the state vector was:

$$\mathbf{x}(t) = [q_1, q_2, \mathrm{d}q_1/\mathrm{d}t, \mathrm{d}q_2/\mathrm{d}t, a_1, a_2, a_3, a_4, a_5, a_6, e_1, e_2, e_3, e_4, e_5, e_6],$$

where q_1 and q_2 are the shoulder and elbow angles, $\mathrm{d}q_1/\mathrm{d}t$ and $\mathrm{d}q_2/\mathrm{d}t$ the shoulder and elbow velocities. The boundary conditions [Eqn (2)] were the initial and final arm postures with zero initial and final velocity, activation and excitation [i.e. $\mathbf{x}(t_0) = x_0$ and $\psi = \mathbf{x}(t_f) - (\mathbf{x}_f)$, where

$$\mathbf{x}_0 = [q_{10}, q_{20}, 0, 0, 0, 0, 0, 0, 0, 0, 0, 0, 0, 0, 0, 0]$$

and

$$\mathbf{x}_f = [q_{1f}, q_{2f}, 0, 0, 0, 0, 0, 0, 0, 0, 0, 0, 0, 0, 0, 0]$$

To simulate isometric force production, the torques were translated into endpoint force (**Φ**) using:

$$T = J(\mathbf{q})^T \Phi,$$

where $T = [T_{sh}\ T_{el}]^T$, and $J(\mathbf{q})$ is the Jacobian matrix of the kinematic transformation at position $\mathbf{q} = [q_1\ \ q_2]^T$. The state vector was $\mathbf{x}(t) = [a_1, a_2, a_3, a_4, a_5, a_6, e_1, e_2, e_3, e_4, e_5, e_6]$.

A force trajectory was specified by initial and final forces (Φ_0 and Φ_f). The boundary conditions were:

$$\mathbf{x}_0 = [a_{10}, a_{20}, a_{30}, a_{40}, a_{50}, a_{60}, e_{10}, e_{20}, e_{30}, e_{40}, e_{50}, e_{60}]$$

and

$$\psi(\mathbf{x}(t_f)) = \mathbf{T}(t_f) - \mathbf{T}_f,$$

where $\mathbf{T}_f = J(\mathbf{q})^T \Phi_f$. For simulations, $(q_1, q_2) = (q_{10}, q_{20})$.

Solution to the optimal control problem

The problem defined by Eqns (1–3) or Eqns (1), (2), (6) and (7) was solved numerically using a gradient method (Bryson, 1999; Guigon *et al*., 2007). The results were obtained as:

$$\mathbf{x}(t_k),\ \mathbf{u}(t_k)[\text{or}\ \mathbf{U}(t_k)]\text{for}\, t_k = t_0 + (t_f - t_0)k/n, \qquad (8)$$

with $k = 0, \ldots, n$, and $n = 50$.

Data analysis

The CSs and NCSs can be considered as inputs to motoneurons [Eqn (4)], and could correspond to activities in subsets of cortical and spinal neurons. They were analysed as if they were the discharge of motor cortical neurons, i.e. by quantifying their directional tuning using regression analysis (Georgopoulos *et al*., 1982). For each NCS, preferred directions (PDs) were calculated at each time step t_k ($0 \le k \le n$). The main PD was defined as PD($t = t_0$). Population vectors were calculated following classical techniques. Bimodal distributions were frequently encountered, and were quantified by a preferred axis as defined by principal component analysis. Electromyographic (EMG) activity was defined as $[e]^+$ [e, excitation; Eqn (5)].

Parameters and comparison with experimental data

The model was built for a direct comparison with experimental data in monkeys (Scott *et al*., 2001; Graham *et al*., 2003; Kurtzer *et al*., 2006). Thus, a number of parameters were directly taken monkey data. Biomechanical parameters (segment inertia I in kg/m^2, mass m in kg, centre of mass cof in percentage of the length, length L in m) were taken from Cheng & Scott (2000) for *Macaca mulatta*. Indexes 1 and 2 are used for upper arm and forearm, respectively. We used $I_1 = 0.00126$, $m_1 = 0.699$, $cof_1 = 0.5$, $L_1 = 0.144$, $I_2 = 0.00621$, $m_2 = 0.781$, $cof_2 = 0.375$, $L_2 = 0.257$. Muscular parameters were taken from Brown *et al*. (1996): $c_2 = -0.02$, $k_2 = -18.7$, $L_{r2} = 0.79$, $\beta = 2.3$, $\omega = 1.26$, $\rho = 1.62$, $a_1 = 0.17$, $b_1 = -0.69$, $b_2 = 1.8$, $a_2 = pL^2 + qL + r$, $p = -5.34$, $q = 8.41$, $r = -4.7$. The muscle time constant was $\upsilon = 0.05$ s (van der Helm & Rozendaal, 2000). The moment arms (Graham & Scott, 2003) are shown in Fig. 1C.

Parameters that are less well defined are the tension scaling factor Γ (Buchanan, 1995), and the PCSAs that depend on the muscles that are actually involved at a given articulation. We chose $\Gamma = 35$ N/cm^2, and the PCSAs were used as free parameters and were adjusted according to the following criteria: (i) each PCSA is in a reasonable range (1–15 cm^2); (ii) movement trajectories have a direction-dependent curvature (fig. 1 in Graham *et al*., 2003); (iii) spatial selectivity of the muscles is as close as possible to that described by Kurtzer *et al*. (2006). Yet, as the model entails a number of simplifications, we thought that the search of an exact fit of the data would be meaningless. Thus, we used a set of PCSAs that provide a good description of experimental observations. The PCSAs (in cm^2) were (for shFL, shEX, elFL, elEX, biFL, biEX): 10, 10, 11, 11, 9.9, 9.9.

For comparison between outcomes of the model and experimental data, we either reproduce an original figure or indicate in the text a reference to one or more published figures.

Results

Properties of planar, 2-DOF reaching movements

Mechanical, muscular and neural characteristics of planar, 2-DOF reaching movements have been thoroughly studied by Scott *et al*. (2001), Graham *et al*. (2003) and Kurtzer *et al*. (2006) (noted Scott, Graham and Kurtzer below). In these experiments, monkeys performed radial reaching movements toward 16 targets. The movement amplitude was 6 cm, and the movement duration was $\sim$600 ms (576 ms in Scott; figs 1 and 2 in Graham; figs 1 and 2 in Kurtzer). The initial posture was approximately (30°, 90°) in Graham and Kurtzer (fig. 2C in Graham; p. 3221 in Kurtzer), but was not reported in Scott. In this latter case, we used (30°, 80°), which provides a good fit to the data. We simulated similar movements with the model, and we obtained movement kinematics (trajectories), movement kinetics (torques, power), muscular activities and NCSs.

Kinematics and kinetics

Trajectories are shown in Fig. 2A, and fig. 1A–C in Graham for comparison. Note that the model accounted for directional variations in movement curvature (see also Guigon *et al*., 2007). The model also reproduced the anisotropy in motion at shoulder and elbow joints (Figs 2B–F; figs 3A, C–F in Graham; fig. 2C in Kurtzer). The kinetic data reported by Graham concerned active torques, i.e. the combination of passive torques generated at shoulder and elbow, and voluntary muscular torques. Active torques were obtained with the model by subtracting modelled passive torques (from fig. 3C and D in Graham) from actual torques generated by the controller. The results are shown in Fig. 3. The model reproduced directional variations in peak active torque (Figs 3A–C; figs 5A–C in Graham; fig. 2C in Kurtzer) and peak joint power (Figs 3D–F; figs 8A–C in Graham). A difference between the experiment and the model was found for the spatio-temporal profile of active shoulder torques (Fig. 3B; fig. 5B in Graham). A possible reason for this difference is related to approximations in the representation of the passive torques. Similar results were obtained with the modified models (NOLV and NOBI).

Muscular activity

Peak muscular activities varied with movement direction (Fig. 4A; fig. 6 in Kurtzer). The monoarticular muscles behave as found experimentally [130–309° (model) vs 130–319° (Kurtzer) axis for the shoulder muscles; 271–73° (model) vs 275–70° (Kurtzer) axis for the elbow muscles]. We could not reproduce the observations of Kurtzer on the activities of the biarticular muscles. The origin of

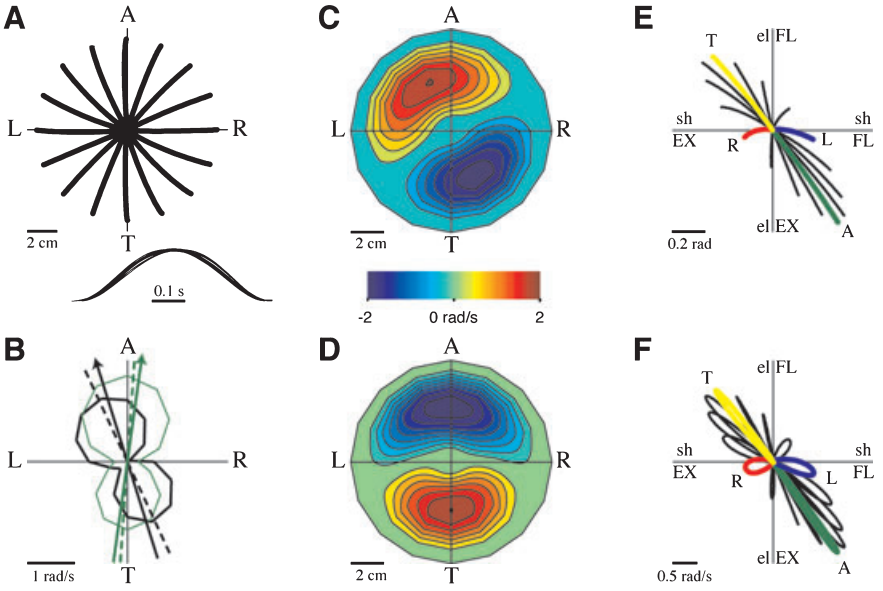

FIG. 2. (A) Trajectories and velocity profiles for movements in 16 directions. R, right; A, away; L, left; T, toward. The initial posture was (30°, 90°). (B) Polar plot of peak shoulder (black line) and elbow (green line) velocity. Arrows indicate the mean bimodal distribution (dashed lines from Graham, fig. 2C). (C) Spatial map of instantaneous angular velocity at shoulder at each location in space along the movement. (D) Same as (C) for elbow velocity. (E) Change in joint angle coordinates. Colours are used to indicate the four cardinal directions. (F) Change in joint velocity in joint angle coordinates.

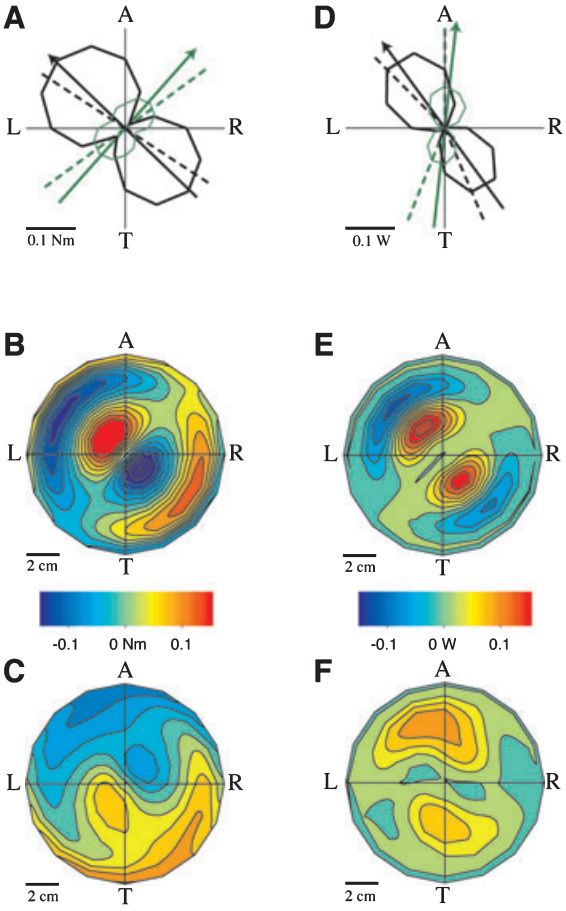

this discrepancy is unclear. We first note that the search over PCSAs has never lead to activities of the biarticular muscles as predicted by Kurtzer. Furthermore, similar results were reported by Li (2006) with a closely related model (her fig. 5.7; see also Todorov & Li, 2005). Thus, our results could hardly be ascribed to some errors in the simulations of the model. To deepen this issue, we have plotted the preferred axis of the six muscular types obtained by Kurtzer in monkeys, by Li (2006) and by us in an optimal control model, and by Welter & Bobbert (2002) in humans (Fig. 4D). We observed that the tuning of the monoarticular muscles is consistent across the studies, but there is a noteworthy discrepancy between Kurtzer and the other studies for the biarticular muscles (* in Fig. 4D). We also note that the model proposed by Kurtzer to explain their data does not reproduce the tuning of the biarticular muscles (their fig. 11C). The discrepancy between the model and the data does not prevent the model explaining the characteristics of NCSs (see below).

NCSs

We analysed the NCSs ($s = 500$) corresponding to movements from initial posture (30°, 80°). We calculated the main PD of each NCS (see Materials and methods), and the distribution of main PDs over the

FIG. 3. (A) Polar plot of peak shoulder (black line) and elbow (green line) torque. Arrows indicate the mean bimodal distribution (dashed lines from Graham, fig. 5A). (B) Spatial map of instantaneous shoulder torque at each location in space along the movement. (C) Same as (B) for elbow torque. (D) Same as (A) for peak shoulder and elbow joint power (dashed lines from Graham, fig. 8). (E) Same as (B) for shoulder joint power. (F) Same as (E) for elbow joint power.

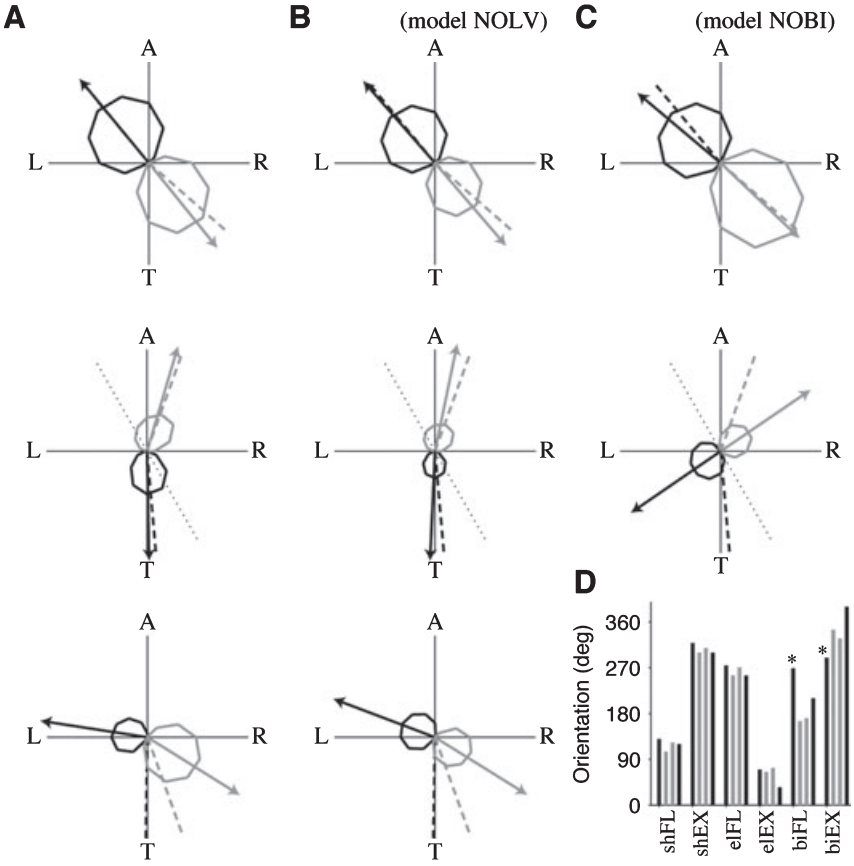

FIG. 4. (A) (Top) Polar plot of peak shoulder muscle flexor (black) and extensor (grey) activity. Arrows indicate the preferred axis of the distribution (dashed lines from Kurtzer, fig. 6). The dashed line for the shoulder flexor is exactly behind the arrow. (Middle) Same as (Top) for the elbow flexor and extensor. (Bottom) Same as (Top) for the biarticular flexor and extensor. (B) Same as (A) for the model NOLV. (C) Same as (A) for the model NOBI. (D) Orientation of the preferred axis of muscles obtained from four sources. For each muscle, four results are given (black: experiment; grey: model). (1) Data of Kurtzer (their fig. 6). (2) Model of Li (2006) (her fig. 5.7c). As the initial posture was (45°, 90°), we subtracted 15° to the reported orientations; (3) Our results (A). (4) Data of Welter & Bobbert (2002) (their fig. 5). As the initial posture was (0°, 90°), we added 30° to the reported orientations. * indicates a noteworthy discrepancy.

NCSs. This distribution was anisotropic with a preferred axis along 123–303° (Fig. 5A; 118–298°, fig. 3 in Scott). The population vector systematically deviated from movement direction (Fig. 5B; fig. 2A in Scott). We explored the relationship between PD distribution and direction-dependent variations in peak angular velocity, peak joint torque and peak joint power. The best correlation was found with peak joint power (Fig. 5D; fig. 4 in Scott).

The PD distribution remained anisotropic for different orientations of the arm and the forearm, and its orientation rotated with both shoulder and elbow angles (Fig. 6A and B). These results can be considered as predictions, as the corresponding experiment has not been performed with a mechanical exoskeleton. Yet, they are consistent with results obtained with other kinematic chains (Caminiti *et al*., 1991; Kakei *et al*., 1999).

Similar results were obtained with the modified models (NOLV and NOBI). However, the correlations with peak joint power were weaker (not shown), and the PD distribution rotated more steeply with elbow angle (Fig. 6B).

Other movements

Complementary information on the nature of NCSs can be found in other studies that analysed the temporal structure of motor cortical discharges during reaching movements and isometric force production (Sergio & Kalaska, 1998; Sergio *et al*., 2005). However, as neither kinematics nor kinetics were quantitatively described in these studies, we only addressed qualitative features of neural discharges. Furthermore, as we found that all the NCSs were qualitatively similar, we only analysed the six CSs (one per muscle).

The raw temporal profile of the shoulder extensor control is shown in Fig. 7 for movements in eight directions (Fig. 7, centre). The control had: (i) an early phasic component followed by a depression for the rightward/downward movements; (ii) a delayed phasic component for a movement in the opposite directions. We note that quantitatively similar results were obtained with the NOLV model (Fig. 7, grey lines). Similar temporal profiles were found for the other muscles, each with its PD tuning (not shown). For comparison with experimental data, we have replotted the control for the shoulder extensor in a different format that can be read as a mean discharge frequency (Fig. 8A). Data from single-unit recording in the primate M1 are reproduced (fig. 1 in Sergio & Kalaska, 1998; Fig. 8B). Visual inspection revealed a close correspondence between real and simulated profiles, although a difference was visible at the end of the movement (see Discussion). We note that the large phasic transient near the end of the movement (Figs 7 and 8A) is due to a strict boundary condition [Eqn (2)]: the movement must finish at a given time and position. This type of boundary condition was chosen for simplicity, but requires large controls to guarantee the exact fulfilment of spatial and temporal constraints. Yet real movements do not in general terminate abruptly,

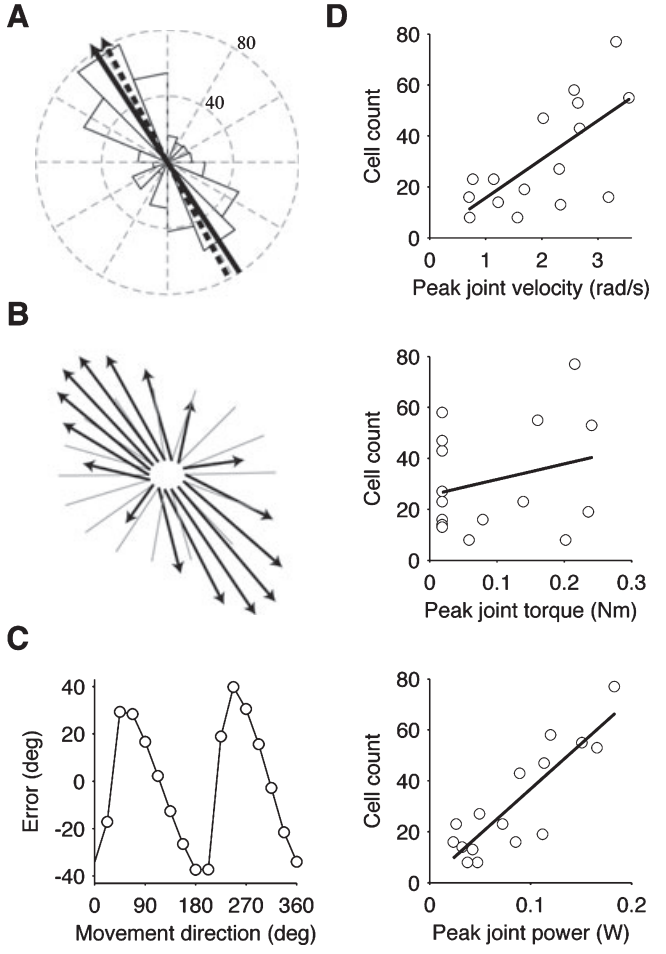

FIG. 5. (A) Frequency distribution of the PDs of the NCS ($s = 500$; mean $R^2 = 0.91$). The radial axis is the number of NCSs in a bin (16 bins, bin size is 22.5°). Solid arrow is the preferred axis of the distribution. Dashed arrow from Scott. (B) Population vector (arrow) vs movement direction (grey) for the 16 directions. (C) Difference between the direction of the population vector and the movement direction as a function of movement direction. (D) Relationship between NCSs count and peak joint velocity (top), peak joint torque (middle) and peak joint power (bottom) for data in (A). The regression line is shown. From top to bottom: $R^2 = 0.46$, 0.07, 0.75.

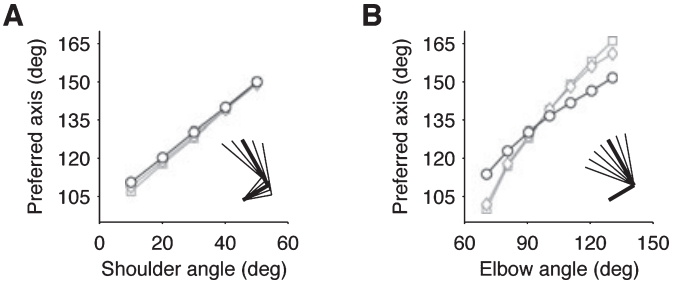

FIG. 6. (A) Preferred axis of the PD distribution as a function of the shoulder angle (10–50°). The elbow angle was 90°. The slope was 0.98 ($R^2 = 1$). Grey lines: results obtained with the model NOLV (square) and the model NOBI (diamond). Inset: initial arm postures. (B) Preferred axis of the PD distribution as a function of the elbow angle (70–130°). The shoulder angle was 30°. The slope was 0.61 ($R^2 = 0.98$). Grey lines: see (A). Inset: initial arm postures.

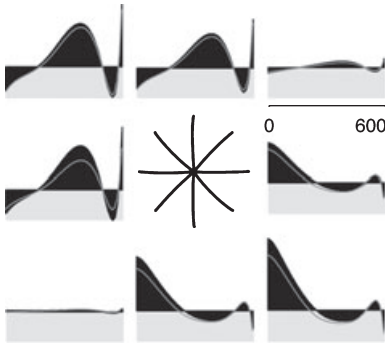

FIG. 7. Temporal profile of the shoulder extensor NCS for movements in eight directions. The NCS is depicted with a black surface, and takes both positive (above the grey surface) and negative (within the grey surface) values. The grey lines are the results obtained with the model NOLV. The time scale is in ms. The trajectories are shown in the middle.

but end up smoothly, e.g. with oscillations. A more realistic movement could be obtained in the presence of noise. In this case, estimated limb position is in general different from actual limb position, so a non-zero residual error should always be present to drive movement corrections. This case is illustrated in fig. 1D of Guigon *et al.* (2007).

For comparison, we applied the model to the production of isometric forces in different directions. Because the calculated CSs are related to dynamic forces, they are not responsible for static force exertion after the dynamic period. To obtain more realistic CSs, we added a static component necessary for the maintenance of a steady final force. For a 150-ms force increase from 0 to 1.5 N, the temporal profile of the shoulder extensor CS had a phasic excitation for a rightward-directed force (Fig. 9A, right) and a phasic inhibition for a leftward force (Fig. 9A, left). Data from single-unit recording in the primate M1 are reproduced (fig. 1 in Sergio & Kalaska, 1998; Fig. 9B).

PDs of the CSs were calculated every 10 ms and displayed in a circular plot (Fig. 10). In the movement task (Fig. 10A; from top to bottom, sh, el, bi; black circle: flexor; grey circle: extensor), the PD reverted during the movement. In contrast, the isometric controls did not revert their PDs (Fig. 10B). For comparison, data from Sergio & Kalaska (1998) are reproduced in Fig. 10C.

Discussion

The present article describes a model-based approach to the nature of NCSs generated by the nervous system of monkeys to control arm movements. The model reproduces detailed features of movement kinematics and kinetics, and quantitative characteristics of single neuron and population discharges in the primate M1. The results support the idea that: (i) the motor system controls movement using a muscle-based controller; (ii) this controller could be located in the motor cortex.

Nature of the model

The model is an optimal controller, i.e. a controller that calculates appropriate CSs to displace a controlled object using a complete knowledge of the properties of the object (here, the dynamics of the arm and the characteristics of the muscles), and an optimality criterion. Recent reviews have thoroughly advocated this type of model to address behavioural and neural characteristics of goal-directed movements (Scott, 2004; Todorov, 2004). We refer the reader to these reviews for a detailed discussion of optimal control models.

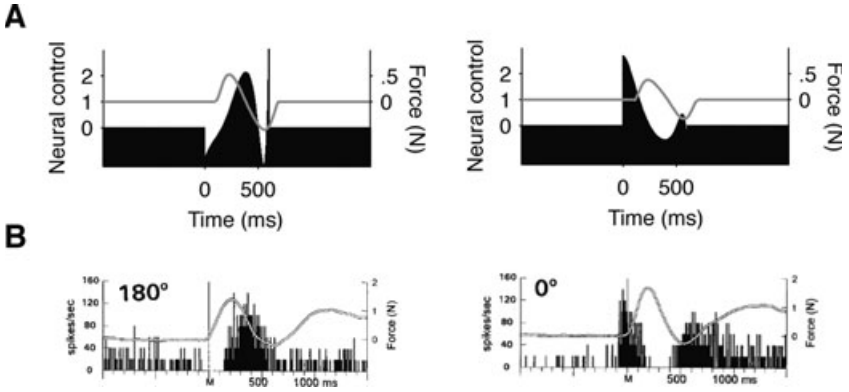

FIG. 8. (A) Temporal profile of the shoulder extensor NCS for a leftward (left) and a rightward (right) movement. Same data as in Fig. 7, but in a different format. Grey line: endpoint force (shifted in time by 100 ms for correspondence with experimental data). (B) Reproduced from Sergio & Kalaska (1998), fig. 1, used with permission.

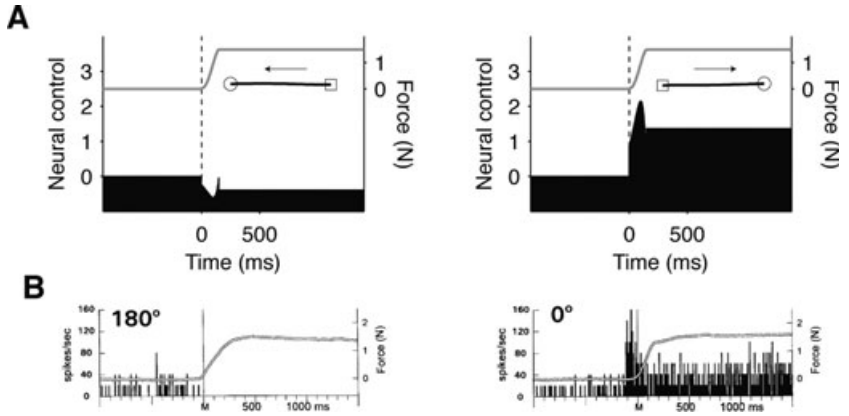

FIG. 9. (A) Same as Fig. 8A for an isometric force production (0–1.5 N in 150 ms). The time course of force variation is shown in grey. Inset: force trajectory (open square: origin; open circle: extremity). (B) Reproduced from Sergio & Kalaska (1998), fig. 1, used with permission.

The present model is not fundamentally different from previous models that applied optimal control techniques to determine the spatio-temporal nature of command signals that should enter a neuromuscular system to drive a limb toward a goal (Happee, 1992; Lan & Crago, 1994; Lan, 1997; Harris & Wolpert, 1998; Haruno & Wolpert, 2005; Todorov & Li, 2005; Li, 2006). A common result of these models is that optimal control of a low-pass filtering force-generating system leads to reasonably realistic EMG and NCSs. The originality of this work is not to describe a new, more efficient model, but to deepen our understanding of neural information processing in the motor cortex using a model-based approach, which proves that observed discharge characteristics of single neurons and populations recorded during movements in M1 can be quantitatively explained by observed characteristics of the movements. In fact, previous models have addressed properties of neurons, but not properties of limb movements (Lan, 1997; Bullock *et al*., 1998; Todorov, 2000; Haruno & Wolpert, 2005; Trainin *et al*., 2007).

Limitations

There are at least three limitations to the present model. First, although the model appropriately produces the expected results, the issue of its validity in a broader framework remains open. The model was actually tested in various conditions, and was found to be consistent with experimental observations (Guigon *et al*., 2007). Yet some data, e.g. highly non-symmetric velocity profiles, cannot be explained by the model. Second, the way optimal feedback control can be computed by brain circuits remains elusive. A third and related limitation is the absence of a relationship between the computational processes advocated by the model and organizational features of the motor cortex (connectivity, intrinsic properties, …). The two latter issues raise the problem of neural information processing subserving motor control. This problem has been addressed for initial directional commands of reaching movements (Baraduc *et al*., 2001), but remains open for the whole spatio-temporal commands.

Motor cortical physiology

Single-cell recordings in M1 have revealed a large repertoire of discharge patterns. In fact, the greater part of movement parameters, ranging from exerted force (low-level muscle control) to serial order of stimuli (cognitive motor control) have been found to influence the discharge of motor cortical neurons (Ashe, 1997; Georgopoulos, 2000). This paradox is hotly debated (Georgopoulos & Ashe, 2000; Moran & Schwartz, 2000; Todorov, 2000). A central issue of the debate is the interpretation of correlation analyses that are used to quantify neuronal activities. For instance, Todorov (2000) defends the view that M1 neurons calculate muscular activation patterns, and

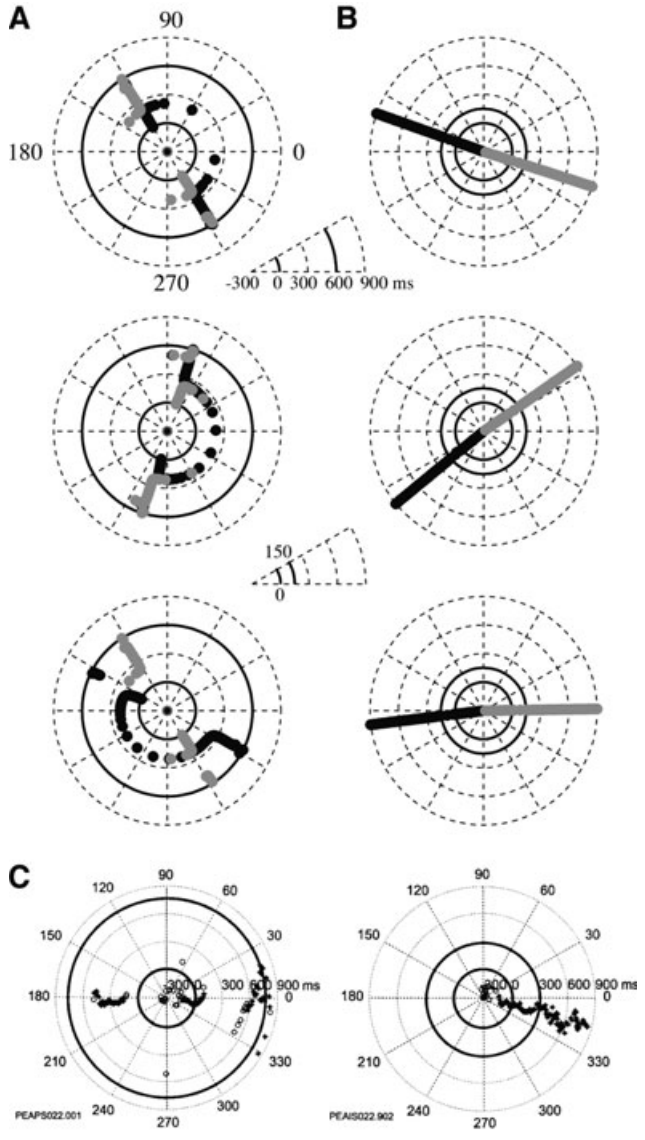

FIG. 10. (A) Time course of PDs of CSs in the reaching task. The time is indicated by the distance from the centre (−300 ms) to the external circle (900 ms). PD is indicated by an angular position. (Top) Shoulder flexor (black), shoulder extensor (grey). (Middle) Elbow flexor (black), elbow extensor (grey). (Bottom) Biarticular flexor (black), biarticular extensor (grey). (B) Same as (A) for the isometric force production task. The two insets indicate the timing for (A) (top inset) and (B) (middle inset). (C) Reproduced from Sergio & Kalaska (1998), fig. 2, used with permission.

suggests that many correlations between kinematic quantities and neural discharges in M1 can be explained by this hypothesis (i.e. they are artefacts). In this framework, a series of studies by Scott and collaborators have attempted to circumvent the weakness of correlation analysis (Scott *et al*., 2001; Graham *et al*., 2003; Kurtzer *et al*., 2006). They reported a systematic description of planar two-joint arm movements and neural correlates of their execution. They found that anisotropic characteristics of movement dynamics and muscular selectivities were associated with a similar anisotropy in neural selectivities. Our model reproduces a similar relationship between mechanical, muscular and neural quantities, and supports the contention of Scott of a tight link between neural populations in M1 and the motor apparatus. The model further shows that the spatio-temporal profile of the NCSs is qualitatively similar to the activity in a subpopulation of motor cortical neurons (located primarily in caudal M1) whose discharge tightly follows the time course of required task dynamics (Sergio & Kalaska, 1998; Sergio *et al*., 2005). Taken together, these results suggest that a subset of M1 neurons could actively participate to a muscle-based representation of movements (Todorov, 2000, 2003; Sergio *et al*., 2005). Although a number of arguments concur to this conclusion (Scott, 1997; Todorov, 2000, 2003), our model provides the first realistic demonstration that muscle-based coding can account simultaneously for movement kinematics, movement kinetics, EMGs and cortical discharges.

If our conclusions are correct, the origin and function of other types of neuron (e.g. those related to visuospatial and kinematic representations of movements) remain to be explained. There are at least two hypotheses. The first is related to the idea of sensorimotor transformations (Kalaska & Crammond, 1992; Scott, 2005). The assumption is that the nervous system performs sequential operations that progressively translate spatial information on the goal of the movement into appropriate commands, going through kinematic, dynamic and muscular stages. In this case, quantities related to desired movement kinematics, in particular desired movement velocity, should be found in M1 (Moran & Schwartz, 1999). This explanation relies on the questionable idea that motor control is based on trajectory tracking (Todorov & Jordan, 2002; Guigon *et al*., 2007). The second hypothesis ensues from the model. As discussed in the Materials and methods, the controller can be considered as an optimal feedback controller, i.e. an optimal controller coupled with a state estimator. We have described properties of the signals elaborated by the controller. Yet other signals should be available to indicate the goal and the estimated state. This latter signal should convey information related to predicted position, velocity, force, etc. Such a predictive (rather than desired) signal could be a source of kinematic information in the motor cortex. For instance, cortical velocity signals have been described in M1 that lead actual velocity by 120–150 ms (Moran & Schwartz, 1999; Wang *et al*., 2007). As the CSs reported in other studies lead movement onset by 100–200 ms (Kalaska *et al*., 1989; Sergio & Kalaska, 1998; Sergio *et al*., 2005), it is possible that the velocity signals derive from the CSs through a forward model. However, these data could also be interpreted to support the presence of a desired velocity signal.

Todorov (2000) has proposed that the dependence of muscle force on length and velocity has a substantial influence on neural information processing in the motor cortex. Kurtzer *et al*. (2006) have suggested that these intrinsic muscular properties are necessary to account for the directional tuning of muscular activities. Our model does not concur with these ideas. First, the temporal profile of our CSs did not resemble a velocity profile (Fig. 2; fig. 7 in Todorov, 2000). In fact, low-pass filtering renders the CSs much more 'phasic' than velocity, even in the presence of a force–velocity relationship in the muscles. Second, muscular tuning was only weakly influenced by force–length and force–velocity relationships (Fig. 4).

According to the separation principle (Guigon *et al*., 2007), a complete motor command involves both a static and a dynamic component. Although such components have been observed experimentally in M1 (Cheney & Fetz, 1980; Kalaska *et al*., 1989; Kurtzer *et al*., 2005), the discharge of many motor cortical neurons appears to carry simultaneously static and dynamic commands (Cheney & Fetz, 1980; Kalaska *et al*., 1989; Sergio & Kalaska, 1998; Kurtzer *et al*., 2005; Sergio *et al*., 2005). For instance, phasic–tonic neurons recorded by Sergio & Kalaska (1998) have an early component that could be related to the control of dynamic forces (compare Fig. 8A and B), and a late component that could be related to the maintenance of posture

against a steady force. In fact, Sergio & Kalaska (1998) have found phasic, tonic and phasic–tonic neurons in equal proportions (∼ 30%), and it is possible that their phasic neurons (not described in detail) are closer to our NCSs than the phasic–tonic neurons. In this case, the phasic and tonic neurons would represent the actual dynamic and static commands as defined by the model. This issue remains to be tested experimentally.

Models of motor control

The debate on the nature of motor cortical representations of movement is part of a more general debate on the nature of motor controllers in the brain (Kawato, 1999; Ostry & Feldman, 2003; Todorov, 2003). On the one hand, position control models exploit viscoelastic properties of muscles and peripheral reflex loops to define limb movements as a series of stable equilibrium postures (Bizzi *et al*., 1992; Feldman & Levin, 1995). The corresponding descending commands can be viewed as kinematic signals as they need not take into account biomechanical or muscular characteristics of the moving limb (Flanagan *et al*., 1993; Georgopoulos, 1996). By construction, the temporal profile of these commands is monotonic. Computer simulations have shown that triphasic EMG patterns can be obtained from monotonic commands that act to modify the recruitment threshold of muscles rather than the force developed by the muscles (St-Onge *et al*., 1997; Suzuki & Yamazaki, 2005). On the other hand, force control models have been developed, based on the idea that the nervous system explicitly computes time-varying CSs to achieve a desired movement (Kawato *et al*., 1987; Uno *et al*., 1989; Todorov, 2000; Franklin *et al*., 2003). Although this type of model has been questioned based on the posture/movement paradox (Ostry & Feldman, 2003), it has proven highly efficient to account for a large range of characteristics of motor control (trajectory formation, EMG). The force control models predict that the NCSs should have non-monotonic (acceleration-like, torque-like, EMG-like) profiles. The present model, which is affiliated to the force control models (in the sense that the CSs are directly transmitted to a force-generating system), shows that the predicted non-monotonic NCSs are quantitatively related to the spatio-temporal characteristics of a population of motor cortical neurons. There is no corresponding study of the CSs predicted by position control models and their relationship to cortical physiology. In particular, the origin and role of non-monotonic discharge patterns in the framework of position control models remain unclear (Todorov, 2003). Although our model cannot directly settle the controversy between force and position control, it gives a physiological basis to the force control models, and contributes to a series of arguments that support these models (Kawato, 1999; Todorov, 2000, 2003; Guigon *et al*., 2007).

Acknowledgement

We thank Marc Maier for fruitful discussions.

Abbreviations

CS, control signal; DOF, degrees of freedom; EMG, electromyographic; M1, primary motor cortex; NCS, neural control signal; PD, preferred direction.

References

Aflalo, T.N. & Graziano, M.S.A. (2006) Partial tuning of motor cortex neurons to final posture in a free-moving paradigm. *Proc. Natl Acad. Sci. USA*, **103**, 2909–2914.

Ashe, J. (1997) Force and the motor cortex. *Behav. Brain Res.*, **87**, 255–269.

Ashe, J. & Georgopoulos, A.P. (1994) Movement parameters and neural activity in motor cortex and area 5. *Cereb. Cortex*, **4**, 590–600.

Baraduc, P., Guigon, E. & Burnod, Y. (2001) Recoding arm position to learn visuomotor transformations. *Cereb. Cortex*, **11**, 906–917.

Bernstein, N. (1967) *The Co-Ordination and Regulation of Movements*. Pergamon Press, Oxford.

Bizzi, E., Hogan, N., Mussa-Ivaldi, F.A. & Giszter, S. (1992) Does the nervous system use equilibrium-point control to guide single and multiple joint movements? *Behav. Brain Sci.*, **15**, 603–613.

van Bolhuis, B.M., Gielen, C.C.A.M. & van Ingen Schenau, G.J. (1998) Activation patterns of mono-and bi-articular arm muscles as a function of force and movement direction of the wrist in humans. *J. Physiol. (Lond.)*, **508**, 313–324.

Brown, I.E., Scott, S.H. & Loeb, G.E. (1996) Mechanics of feline soleus. II. Design and validation of a mathematical model. *J. Muscle Res. Cell. Motil.*, **17**, 221–233.

Bryson, A.E. (1999) *Dynamic Optimization*. Prentice Hall, Englewood Cliffs, NJ.

Buchanan, T.S. (1995) Evidence that maximum muscle stress is not a constant: differences in specific tension in elbow flexors and extensors. *Med. Engng Phys.*, **17**, 529–536.

Bullock, D., Cisek, P. & Grossberg, S. (1998) Cortical networks for control of voluntary arm movements under variable force conditions. *Cereb. Cortex*, **8**, 48–62.

Bullock, D. & Grossberg, S. (1988) Neural dynamics of planned arm movements: emergent invariance and speed-accuracy properties during trajectory formation. *Psychol. Rev.*, **95**, 49–90.

Caminiti, R., Johnson, P.B., Galli, C., Ferraina, S. & Burnod, Y. (1991) Making arm movements within different parts of space: the premotor and motor cortical representation of a coordinate system for reaching to visual targets. *J. Neurosci.*, **11**, 1182–1197.

Cheney, P.D. & Fetz, E.E. (1980) Functional classes of primate corticomotoneuronal cells and their relation to active force. *J. Neurophysiol.*, **44**, 773–791.

Cheng, E.J. & Scott, S.H. (2000) Morphometry of Macaca mulatta forelimb. I. Shoulder and elbow muscles and segment inertial parameters. *J. Morph.*, **245**, 206–224.

Evarts, E.V. (1968) Relation of pyramidal tract activity to force exerted during voluntary movement. *J. Neurophysiol.*, **31**, 14–27.

Feldman, A.G. & Levin, M.F. (1995) The origin and use of positional frames of reference in motor control. *Behav. Brain Sci.*, **18**, 723–744.

Fetz, E.E. (1992) Are movement parameters recognizably coded in the activity of single neurons? *Behav. Brain Sci.*, **15**, 679–690.

Flanagan, J.R., Ostry, D.J. & Feldman, A.G. (1993) Control of trajectory modifications in target-directed reaching. *J. Mot. Behav.*, **25**, 140–152.

Franklin, D.W., Osu, R., Burdet, E., Kawato, M. & Milner, T.E. (2003) Adaptation to stable and unstable dynamics achieved by combined impedance control and inverse dynamics model. *J. Neurophysiol.*, **90**, 3270–3282.

Fu, Q.G., Flament, D., Coltz, J.D. & Ebner, T.J. (1995) Temporal encoding of movement kinematics in the discharge of primate primary motor and premotor neurons. *J. Neurophysiol.*, **73**, 836–854.

Georgopoulos, A.P. (1996) On the translation of directional motor cortical commands to activation of muscles via spinal interneuronal systems. *Cogn. Brain Res.*, **3**, 151–155.

Georgopoulos, A.P. (2000) Neural aspects of cognitive motor control. *Curr. Opin. Neurobiol.*, **10**, 238–241.

Georgopoulos, A.P. & Ashe, J. (2000) One motor cortex, two different views. *Nat. Neurosci.*, **3**, 963.

Georgopoulos, A.P., Kalaska, J.F., Caminiti, R. & Massey, J.T. (1982) On the relations between the direction of two-dimensional arm movements and cell discharge in primate motor cortex. *J. Neurosci.*, **2**, 1527–1537.

Graham, K.M., Moore, K.D., Cabel, D.W., Gribble, P.L., Cisek, P. & Scott, S.H. (2003) Kinematics and kinetics of multijoint reaching in nonhuman primates. *J. Neurophysiol.*, **89**, 2667–2677.

Graham, K.M. & Scott, S.H. (2003) Morphometry of *Macaca mulatta* forelimb. III. Moment arm of shoulder and elbow muscles. *J. Morph.*, **255**, 301–314.

Guigon, E., Baraduc, P. & Desmurget, M. (2007) Computational motor control: redundancy and invariance. *J. Neurophysiol.*, **97**, 331–347.

Happee, R. (1992) Time optimality in the control of human movements. *Biol. Cybern.*, **66**, 357–366.

Harris, C.M. & Wolpert, D.M. (1998) Signal-dependent noise determines motor planning. *Nature*, **394**, 780–784.

Haruno, M. & Wolpert, D.M. (2005) Optimal control of redundant muscles in step-tracking wrist movements. *J. Neurophysiol.*, **94**, 4244–4255.
van der Helm, F.C.T. & Rozendaal, L.A. (2000) Musculoskeletal systems with intrinsic and proprioceptive feedback. In Winters, J.M. & Crago, P.E. (Eds), *Biomechanics and Neural Control of Posture and Movement*. Springer, New York, pp. 164–174.
Kakei, S., Hoffman, D.S. & Strick, P.L. (1999) Muscle and movement representations in the primary motor cortex. *Science*, **285**, 2136–2139.
Kalaska, J.F., Cohen, D.A.D., Hyde, M.L. & Prud'homme, M. (1989) A comparison of movement direction-related versus load direction-related activity in primate motor cortex, using a two-dimensional reaching task. *J. Neurosci.*, **9**, 2080–2102.
Kalaska, J.F. & Crammond, D.J. (1992) Cerebral cortical mechanisms of reaching movements. *Science*, **255**, 1517–1522.
Kawato, M. (1999) Internal models for motor control and trajectory planning. *Curr. Opin. Neurobiol.*, **9**, 718–727.
Kawato, M., Furukawa, K. & Suzuki, R. (1987) A hierarchical neural network model for control and learning of voluntary movements. *Biol. Cybern.*, **57**, 169–185.
Kurtzer, I., Herter, T.M. & Scott, S.H. (2005) Random change in cortical load representation suggests distinct control of posture and movement. *Nat. Neurosci.*, **8**, 498–504.
Kurtzer, I., Herter, T.M. & Scott, S.H. (2006) Nonuniform distribution of reach-related and torque-related activity in upper arm muscles and neurons of primary motor cortex. *J. Neurophysiol.*, **96**, 3220–3230.
Lan, N. (1997) Analysis of an optimal control model of multi-joint arm movements. *Biol. Cybern.*, **76**, 107–117.
Lan, N. & Crago, P.E. (1994) Optimal control of antagonistic muscle stiffness during voluntary movements. *Biol. Cybern.*, **71**, 123–135.
Li, W. (2006) Optimal control for biological movement systems. Unpublished doctoral Dissertation. University of California, San Diego [http://www.cogsci.ucsd.edu/~todorov/papers/LiThesis.pdf].
Moran, D.W. & Schwartz, A.B. (1999) Motor cortical representation of speed and direction during reaching. *J. Neurophysiol.*, **82**, 2676–2692.
Moran, D.W. & Schwartz, A.B. (2000) One motor cortex, two different views. *Nat. Neurosci.*, **3**, 963.
Mussa-Ivaldi, F.A. (1988) Do neurons in the motor cortex encode movement direction? An alternative hypothesis. *Neurosci. Lett.*, **91**, 106–111.
Ostry, D.J. & Feldman, A.G. (2003) A critical evaluation of the force control hypothesis in motor control. *Exp. Brain Res.*, **153**, 275–288.
Scott, S.H. (1997) Comparison of onset time and magnitude of activity for proximal arm muscles and motor cortical cells before reaching movements. *J. Neurophysiol.*, **77**, 1016–1022.
Scott, S.H. (2004) Optimal feedback control and the neural basis of volitional motor control. *Nat. Rev. Neurosci.*, **5**, 532–546.
Scott, S.H. (2005) Conceptual frameworks for interpreting motor cortical function: new insights from a planar multiple-joint paradigm. In Riehle, A. & Vaadia, E. (Eds), *Motor Cortex in Voluntary Movements*. CRC Press, London, pp. 157–180.
Scott, S.H., Gribble, P.L., Graham, K.M. & Cabel, W. (2001) Dissociation between hand motion and population vectors from neural activity in motor cortex. *Nature*, **413**, 161–165.
Sergio, L.E., Hamel-Paquet, C. & Kalaska, J.F. (2005) Motor cortex neural correlates of output kinematics and kinetics during isometric-force and arm-reaching tasks. *J. Neurophysiol.*, **94**, 2353–2378.
Sergio, L.E. & Kalaska, J.F. (1998) Changes in the temporal pattern of primary motor cortex activity in a directional isometric force versus limb movement task. *J. Neurophysiol.*, **80**, 1577–1583.
St-Onge, N., Adamovich, S.V. & Feldman, A.G. (1997) Control processes underlying elbow flexion movements may be independent of kinematic and electromyographic patterns: experimental study and modelling. *Neuroscience*, **79**, 295–316.
Suzuki, M. & Yamazaki, Y. (2005) Velocity-based planning of rapid elbow movements expands the control scheme of the equilibrium point hypothesis. *J. Comp. Neurosci.*, **18**, 131–149.
Todorov, E. (2000) Direct cortical control of muscle activation in voluntary arm movements: a model. *Nat. Neurosci.*, **3**, 391–398.
Todorov, E. (2003) On the role of primary motor cortex in arm movement control. In Latash, M.L. & Levin, M.F. (Eds), *Progress in Motor Control III*, Human Kinetics, Champaign, IL, pp. 125–166.
Todorov, E. (2004) Optimality principles in sensorimotor control. *Nat. Neurosci.*, **7**, 907–915.
Todorov, E. & Jordan, M.I. (2002) Optimal feedback control as a theory of motor coordination. *Nat. Neurosci.*, **5**, 1226–1235.
Todorov, E. & Li, W. (2005) A generalized iterative LQG method for locally-optimal feedback control of constrained nonlinear stochastic systems. In *Proceedings of the 2005 American Control Conference*, **Vol. 1**, pp. 300–306.
Trainin, E., Meir, R. & Karniel, A. (2007) Explaining patterns of neural activity in the primary motor cortex using spinal cord and limb biomechanics models. *J. Neurophysiol.*, **97**, 3736–3750.
Uno, Y., Kawato, M. & Suzuki, R. (1989) Formation and control of optimal trajectory in human multijoint arm movement – minimum torque change model. *Biol. Cybern.*, **61**, 89–101.
Wang, W., Chan, S.S., Heldman, D.A. & Moran, D.W. (2007) Motor cortical representation of position and velocity during reaching. *J. Neurophysiol.*, **97**, 4258–4270.
Welter, T.G. & Bobbert, M.F. (2002) Initial muscle activity in planar ballistic arm movements with varying external force directions. *Motor Control*, **6**, 32–51.
Zajac, F.E. (1989) Muscle and tendon: models, scaling, and application to biomechanics and motor control. *Crit. Rev. Biomed. Engng*, **17**, 359–415.